ORGANISED MOTION AND RADIATIVE PERTURBATIONS IN THE NOCTURNAL CANOPY SUBLAYER ABOVE AN EVEN-AGED PINE FOREST

D. CAVA
CNR – Institute of Atmosphere Sciences and Climate – section of Lecce, Italy

U. GIOSTRA
Environmental Science Department, University of Urbino, Italy

M. SIQUEIRA and G. KATUL
Nicholas School of the Environment and Earth Sciences, Duke University, Durham, NC, U.S.A.

(Received in final form 11 August 2003)

Abstract. Using time series measurements of velocity, carbon dioxide and water vapour concentration, and temperature collected just above a 15 m tall even-aged pine forest, we quantify the role of organized motion on scalar and momentum transport within the nocturnal canopy sublayer (CSL). We propose a framework in which the nocturnal CSL has two end-members, both dominated by organised motion. These end-members represent fully developed turbulent flows at near-neutral or slightly stable stratification and no turbulence for very stable stratification. Our analysis suggests that ramps dominate scalar transport for near-neutral and slightly stable conditions, while linear canopy waves dominate the flow dynamics for very stable conditions. For intermediate stability, the turbulence is highly damped and often dominated by fine scale motions. Co-spectral analysis suggests that ramps are the most efficient net scalar mass-transporting agent while linear canopy waves contribute little to net scalar transport between the canopy and atmosphere for averaging intervals that include complete wave cycles. However, canopy waves significantly contribute to the spectral properties of the scalar time series. Ramps are the most frequently occurring organised motion in the nocturnal CSL for this site. Numerous night-time runs, however, resided between these two end-members. Our analysis suggests that when radiative perturbations are sufficient large ($>$20 W m^{-2} in net radiation), the flow can switch from being highly damped fine-scale turbulence to being organized with ramp-like properties. We also found that when ramps are already the dominant eddy motion in the nocturnal CSL, radiative perturbations have a minor impact on scalar transport. Finally, in agreement with previous studies, we found that ramps and canopy waves have comparable length scales of about 30–60 metres. Consequences to night-time flux averaging are also discussed.

Keywords: Canopy waves, CO_2 transport, Nocturnal canopy sublayer, Organized motion, Radiative perturbations, Ramps.

1. Introduction

Over the past decade, the use of eddy-covariance flux towers to monitor vertical carbon dioxide (CO_2) and water vapour (q) fluxes from different biomes has proliferated. Continental networks such as Euroflux (Valentini et al., 2000), AmeriFlux (Baldocchi et al., 2001), and global networks such as FluxNet (Baldocchi et al.,

Boundary-Layer Meteorology **112:** 129–157, 2004.

2001) are now used to monitor annual carbon uptake across a wide range of ecosystems and climate regimes. An emerging uncertainty in quantifying carbon cycling from such flux tower programs, when compared to other standard ecological carbon pool increment methods, is quantifying night-time ecosystem respiration (Falge et al., 2002). To make progress on such issues, it is imperative that the structure of turbulence in the nocturnal canopy sublayer (CSL) be studied in greater detail. One reason why, historically, the nocturnal CSL has not received much attention in micrometeorology, at least when compared to its daytime counterpart, is that latent heat and sensible heat fluxes are relatively small (or negligible).

Daytime CSL turbulence has been the subject of numerous micrometeorological studies (Raupach and Thom, 1981; Bergström and Högstrom, 1989; Gao et al., 1989; Shaw et al., 1989, Paw U et al., 1992; Collineau and Brunet, 1993; Raupach et al., 1996). These studies unequivocally highlighted the role of large and intermittent coherent structures in CSL momentum and scalar transport. Coherent structures in scalar concentration or temperature time series appear as approximate periodic ramps commonly connected with the ejection-sweep cycle (Paw U et al., 1992; Gao et al., 1989; Katul et al., 1997; Finnigan, 2000). The phenomenology of the onset of coherent structures just above dense plant canopies, at least in the simplest cases of planar homogeneous and stationary flows, can be explained through an analogy to Kelvin–Helmholtz instabilities observed in plane mixing layers (Raupach et al., 1996; Finnigan, 2000). Most studies that supported the mixing-layer analogy hypothesis were conducted within and above dense canopies under neutral or mildly unstable conditions (e.g., Raupach et al., 1996; Katul et al., 1998; Brunet and Irvine, 2000). How this emerging picture about organised motion for the neutral CSL is altered by nocturnal conditions is a key question. The issue is driven, in part, by numerous observations that nocturnal CO_2 fluxes, a measure of ecosystem respiration, are often comparable in magnitude to their daytime counterpart (Lee et al., 1996; Lee, 1997; Baldocchi et al., 2001; Lai et al., 2002).

The stable boundary layer is complicated by numerous phenomena including ‘external’ intermittency, and non-turbulent phenomena such as meandering or wavy motions (e.g., Nappo, 1991; Mahrt, 1999). Moreover radiative effects on turbulent transport appear much more significant during nocturnal conditions when compared to their daytime counterpart (Garratt, 1992, p. 164). Despite such complications, numerous plant canopy turbulence experiments have demonstrated a high degree of periodicity in the time series of velocity and scalars (Fitzjarrald and Moore, 1990; Paw U et al., 1992; Brunet and Collineau, 1994; Lee et al., 1996, 1997; Lee, 1997; Lee and Barr, 1998). Periodic inverse ramps or wavelike signals in scalar time series clearly reveal organised structures within and above the forest during nocturnal conditions.

Gravity waves (often called canopy waves) of various intensities have also been frequently observed in a variety of nocturnal CSL experiments. Over the last decade, experimental and theoretical studies both suggest that they play an important

role in nocturnal canopy flow and spectral dynamics (e.g., Lee et al., 1996, 1997). Their role in scalar fluxes remains an active research question (Finnigan, 2000) and is a major thrust of our study. Observed canopy waves exhibit characteristics very different from gravity waves generated in the upper boundary layer (hereinafter, upper gravity waves). They possess a dominant wave period of the order of 60–100 sec, i.e., a period much shorter than that of upper gravity waves; they often possess a single dominant period, while upper gravity waves are rarely monochromatic (de Baas and Driedonks, 1985); and they posses a low phase speed.

A number of studies have also reported synchronous occurrences of inverted ramps near the canopy top and of canopy waves above, both characterised by comparable periods (Paw U et al., 1992; Lee et al., 1996, 1997). All these features suggest that canopy waves may be produced by Kelvin–Helmoltz instabilities induced by the strong wind shear at the canopy top, (i.e., the same mechanism invoked by Raupach et al. (1996) for the generation of the daytime coherent structures). In fact, a recent two-dimensional numerical study by Hu et al. (2002) proposed a four-stage idealised life cycle for the canopy waves: initiation, growth, saturation and destruction. Their study assumes that the source of disturbance is located near the tree top, and during the wave saturation phase sweep-ejection patterns can appear within the core of canopy waves. The latter result may explain why simultaneous occurrences of inverted ramps and waves at different levels above a plant canopy can co-exist.

Other studies have also reported that canopy waves can account for significant co-gradient or counter-gradient fluxes of heat and scalars at night (Fitzjarrald and Moore, 1990; Lee et al., 1996, 1997). Yet these observed waves were not pure linear waves, as the phase angle between vertical wind component (w) and scalars deviated from $\pm 90^{\circ}$ (the expected angle for linear gravity waves).

It is these findings that motivated us to evaluate, via time series analysis, key phenomenological processes affecting momentum and scalar transport near the canopy top in the nocturnal CSL. This study primarily focuses on identifying the relative importance of both inverted ramps and canopy waves on nocturnal momentum and scalar transfer within the CSL. What distinguishes this study from previous efforts is that we investigate how cloud passage induces thermal perturbations that can alter the flux-transporting properties of organised eddy motion. The role of radiative perturbations on the structure of the nocturnal CSL has rarely been studied.

Throughout, we use both index and meteorological notations (i.e., $u_1 = u$, $u_2 = v$, and $u_3 = w$, $x_1 = x$, $x_2 = y$, and $x_3 = z$) with x, y, and z representing longitudinal, lateral, and vertical directions, respectively. The u, v, and w represent velocity components in the x, y, and z directions, respectively. The z direction is referenced to the ground surface or forest floor. The velocity components were rotated in a streamline coordinate system so that the mean lateral velocity is zero (McMillen, 1988). An overbar represents time-averaged quantities, and primed quantities are instantaneous excursions from these averaged quantities.

2. Experiment

Much of the site and experimental set-up is described in Lai et al. (2002) and Siqueira et al. (2002). However, a summary description is provided for completeness. Measurements were conducted at the Blackwood Division of the Duke Forest near Durham, North Carolina (36°2′ N, 79°8′ W, elevation = 163 m) in the U.S.A. The site is a uniformly planted loblolly pine forest (*Pinus taeda L.*), extending 300–600 m in the east-west direction, and 1000 m in the north-south direction and is part of a long-term flux monitoring initiative known as AmeriFlux. The mean canopy height (h) was 15.5 m ($\pm$0.5 m) at the time of the experiment, in June–July of 2001. The topographic variations are small (terrain slope changes $<5\%$) so that the influence of topography on flow statistics can be neglected.

The momentum, CO_2, latent and sensible heat fluxes were measured by an eddy-covariance system, comprising an open path CO_2/H_2O infrared gas analyzer (Licor-7500, LI-COR, Lincoln, NE), and a triaxial sonic anemometer (CSAT3, Campbell Scientific, Logan, UT). The anemometer and the gas analyzer were positioned 16.5 m above the forest floor. A Fritchen-type net radiometer was installed at the same height to measure net radiation (R_n). All signals, including R_n, were recorded at 5 Hz using a Campbell Scientific 23X data logger. The data were transmitted via a fibre optic line to a personal desktop computer in a nearby shed for future processing.

3. Method of Analysis

The data analysed derive from 21 evening runs collected between June 27 to July 19, 2001. For each evening, the analysis was restricted to periods from 2000 to 0400 (standard local time). Spikes as well as runs with wind directions contaminated by tower distortions were discarded before performing the analysis discussed below.

3.1. Data classification

The first step in our analysis is detection and identification of the occurrence of organised structures in the flow. Here, we sought geometric attributes (e.g., sinusoidal signals or ramps) that were quasi-periodic and occurred simultaneously in the time series of temperature (T), water vapour (q) and CO_2 concentration. To a first order, ramps are associated with the classical ejection-sweep cycle whereas sinusoidal signals are associated with canopy waves.

Organised events (ramps and waves) have been identified and separated from fine-scale turbulence using a wavelet-based thresholding method that utilizes a Lorentz filter (Katul and Vidakovic, 1998). This detection method is capable of isolating organized events responsible for much of the variances of signals from

fine-scale turbulence. To discriminate between ramps and other wavelike motions (characterised by similar amplitudes and similar period), we used visual identification. Visual identification is considered the method by which all other 'automatic' detection methods must be verified against (Paw U et al., 1992; Shaw et al., 1989). While it is desirable to automate the detection process of such organized motions, we note that 'non-ideal' ramps and waves that are intermittent and non-periodic can lead to 'false detection'. Given the study objectives, we opted to use the most laborious and accurate method of identification: visual inspection.

Ramps (strongly asymmetric structures) were distinguished from wavelike motions (symmetric patterns) when the abrupt scalar time series rise (for temperature) or fall (for humidity and CO_2) occurred in a time interval of few seconds, and when the rise and fall are synchronous in all three scalar signals.

We also verified if passage of clouds (identified by rapid net radiation change greater than 10 W m^{-2}) can disturb the stable boundary layer near the forest. Towards this end, we visually checked the scalar time series for the initiation of organised structures (i.e., ramps or canopy waves) co-occurring with rapid R_n variations. Moreover, to test if the passage of clouds strengthened (or dampened) organised patterns already existing in the flow, we computed the ratio between the 15-min variances of scalar tracers after and before the rapid R_n increase was observed. We selected periods characterised by scalar pattern perturbations correlated with the passage of clouds by checking if the variance-ratio was greater than a threshold value set to 1.5 before and after the R_n change. The 15-min interval for such a calculation was an optimum balance between the need for a short period to assess the scalar perturbations following rapid cloud passages and a sufficiently long period for reliably computing variances.

Following these criteria, we identified and classified the portion of the time series dominated by canopy waves or by ramps. Periods that lacked any geometric organisation or periodicity were classified as fine-structure turbulence. Moreover we detected and identified cases in which the R_n variation significantly perturbed the state of the nocturnal CSL near the canopy-atmosphere interface. The spectral and cospectral properties of all these classes of nocturnal CSL turbulence are considered next.

3.2. Spectral and cross-spectral analysis

The physical characteristics of selected structures, such as canopy waves or ramps, can be obtained via spectral and cross-spectral analysis reviewed below. The power spectrum of an arbitrary flow variable a (S_a) is the Fourier Transform of the a-autocorrelation function (see Subsection 3.3) and its integral is the a-variance:

$$\overline{a'^2} = \sigma_a^2 = \int S_a(f)\,\mathrm{d}f, \tag{1}$$

where f is the natural frequency in Hz and $a = \bar{a} + a'$. The cross-spectrum between two flow variables a and b is the Fourier Transform of the a and b cross-correlation

function (Jenkins and Watts, 1968). The real part of this transformation is called cospectrum (C_{ab}) and its integral represents the a and b covariance:

$$\overline{a'b'} = \int C_{ab}(f)\,\mathrm{d}f. \tag{2}$$

The imaginary part (Q_{ab}) is called the quad-spectrum (or quadrature) and represents the spectrum of the product of a and b shifted by 90°. The phase spectrum is defined as:

$$\phi_{ab}(f) = \tan^{-1}(Q_{ab}(f)/C_{ab}(f)), \tag{3}$$

and represents the phase difference between the a and b time series that yields the greatest correlation for each frequency f (Stull, 1988, p. 332). Via these techniques, we seek to assess whether the commonly observed canopy waves are pure linear waves. The discrimination between linear and non-linear waves is of practical importance in scalar transport. Linear waves do not contribute to the net transport of heat and mass but non-linear waves may contribute.

Normalised velocity spectra ($fS(f)\sigma^{-2}$) measured in the atmospheric surface layer (ASL) above flat and uniform terrain exhibit a number of universal attributes: the position of the spectral peak can be related to the dimension of the energy-containing eddies. The inertial-subrange eddies are locally homogeneous, isotropic, and follow a $-2/3$ power law (Kolmogorov, 1941). In the CSL, the turbulent spectral peak can be related to the dimension of the large coherent structures, which, for unstable and near-neutral conditions, is connected to the size of the Kelvin–Helmholtz instabilities (Raupach et al., 1996; Katul et al., 1998; Brunet and Irvine, 2000). Furthermore, wake and waving production processes alter the classical energy cascade near the canopy. This mechanism produces departures from classical locally isotropic predictions for the longitudinal velocity spectra (S_u) in almost all cases. These departures are associated with more rapid roll-off than $-2/3$, while observations of lateral and vertical spectra are more varied (Finnigan, 2000). We seek to compare these canonical spectral attributes of CSL and ASL turbulence with the measured nocturnal spectral attributes in this study.

Cross-spectral properties of turbulence are strongly related to its diffusive and chaotic character: cospectrum measurements exhibit a peak in the energy-containing region and they are stronger or comparable to the quadrature spectrum; moreover the phase angles are randomly distributed between $-\pi$ and $+\pi$ (giving a mean value near zero). When linear gravity waves are present, the spectra and cross-spectra exhibit peaks associated with high levels of coherence and stable phase angles.

In the wave-source region, the spectral energy rolls off following a -2 power law at frequencies higher than the characteristic wave frequency (Stull, 1988, p. 532). The slope of the spectra in the buoyancy subrange provides a good indication that the peak is attributed to a wave motion and does not reflect some ‘input scale’ of turbulent energy (Caughey and Readings, 1975).

Cross-spectra of vertical velocity component and passive scalars are often used as indicators of wave activity (Bush, 1969; Stewart, 1969; Caughey, 1977; Nai-Ping et al., 1983; Hunt et al., 1985; de Baas and Driedonks, 1985; Smedman, 1988; Bergström and Smedman, 1994). One distinct feature of a pure linear wave field, when compared to turbulence, is the lack of vertical diffusion. In the wave source region the fluctuations of w and any scalar are 90° out of phase. Hence, the quad-spectrum is larger than the cospectrum and the phase spectrum approaches values close to ±90°. In summary, the cospectral properties clearly distinguish between linear waves and turbulence in the absence of non-linear interaction between them.

Fourier transformations are used on the 15-min selected runs, then ensemble averaged. The choice of the temporal period (15 min) is dictated by the patchiness and short persistence (less than 15 min) of observed canopy waves. Nevertheless, it is sufficient to resolve organised structures characteristic of the flow within the roughness sub-layer. Prior to the transformation, low-frequency oscillations and trends have been removed from signals using a cut-off frequency of 10^{-3} Hz to reduce the low-frequency red noise; then the signals are tapered using a Hanning window (Press et al., 1992). Ensemble spectra and cross-spectra are then computed and compared.

3.3. Autocorrelation function and integral time scale

Wave periods and ramp characteristic time scales estimated from the spectral analysis are also compared with the integral time scale obtained from the autocorrelation function. Namely, the integral time scale of a is defined as

$$T_a = \int_0^\infty R_a(\tau)\,\mathrm{d}\tau, \tag{4}$$

where R_a represents the a-autocorrelation function defined as

$$R_a(\tau) = \int_0^\infty \frac{a'(t)a'(t+\tau)}{\sigma_a^2}\,\mathrm{d}t. \tag{5}$$

The integral time scales and autocorrelation functions of longitudinal and vertical wind velocity components and of scalars (T, q and CO_2) are computed on the 15-min selected datasets. Then the average integral time scales and autocorrelation functions of the different detected events are compared. We note that the slow decay and evidence of oscillation in the w-autocorrelation function are often signatures of wave activity (Hunt et al., 1985; Bergström and Smedman, 1994).

4. Results and Discussion

We address the study objectives by first classifying the runs with respect to the type of dominant organised motion (e.g., ramps, canopy waves) if any, and noting whether the sky conditions were clear or cloudy. We progress to compute the ensemble spectral and cospectral properties, as well as auto-correlation, cross-correlation, and integral time statistical values. A discussion is then presented as to how these statistical properties differ from their neutral canopy CSL counterpart, and to what extent radiative perturbations play a role in modulating them in the nocturnal CSL.

4.1. Detection of organised motion

The data were classified into one of the five classes: periods characterised by 'cloud free' conditions with near constant Rn and ramps (class I), canopy waves (class II), and fine-structure turbulence (class III). Periods characterised by cloudy conditions in which R_n variations exceed 10 W m^{-2} and induce (or intensify) organised motion (class IV); and periods characterised by R_n variation greater that 10 W m^{-2}, but not showing any organised perturbation in the scalar time series (class V). Table I lists the frequency of occurrence of these five classes during each night.

Ramps are the structures most frequently observed during the study period (class I is characterised by the highest mean percentage of occurrence, close to 50%). Figure 1 shows a representative time series dominated by ramps. The usual abrupt rise in T, coincident with abrupt drops in CO_2 and q, clearly suggests that the traditional ejection-sweep cycle is most active here. Note the different ramp 'orientation' of T when compared to CO_2 (or q). These differences are attributed to the canopy being a sink of heat while being a source of CO_2 (or q).

Wave-like motion (see Figure 2) was also observed (class II) though much less frequently than ramp patterns. Their mean percentage of occurrence is about 6%: actually their 'time of residence' during each night is extremely variable (from 1.5% to 45%) and in about 50% of the nights analysed, they were completely absent. Canopy waves tend to occur in very stable atmospheric conditions ($z/L \gg 1$, being the Obukhov length) and during low winds (see, for example, mean velocities during ramp and wave episodes shown in Figures 1 and 2). Observed waves are characterised by variable amplitude and by a dominant period of 60–120 sec; moreover they have a short persistence cycle of about 2 to 5 waves before their dissipation.

Figure 3 displays a period representative of flow lacking any large-scale organisation or periodicity and appears to be primarily dominated by fine-scale turbulence. These periods are characterized by low values of u and highly damped velocity and scalar concentration fluctuations.

The analysis of periods subject to large night-time R_n variability (i.e., related to variability in cloud cover) revealed only six cases in which production or intensific-

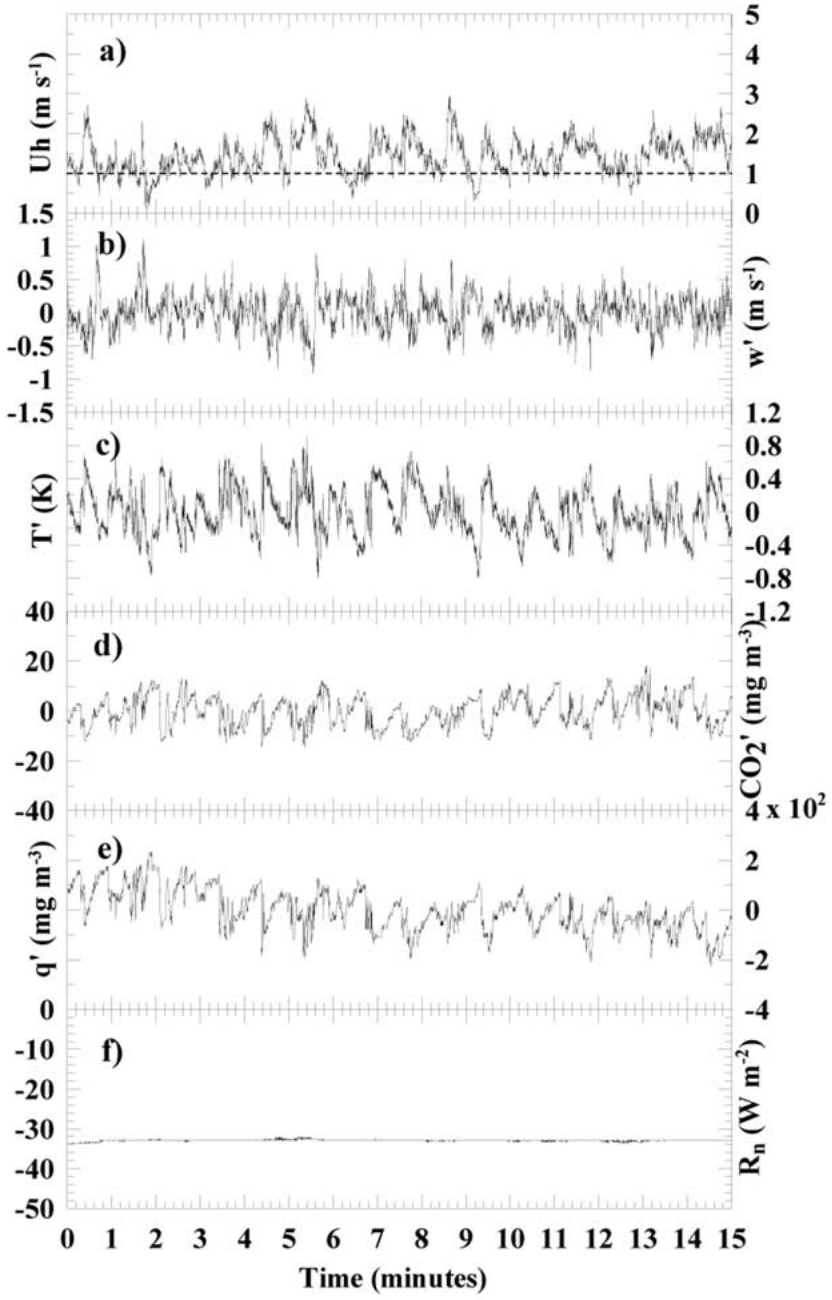

Figure 1. Example time series for class I of (a) horizontal wind velocity component (u) at the canopy top (Uh), (b) vertical wind velocity fluctuations (w'), (c) temperature fluctuations (T'), (d) CO_2 fluctuations, (e) water vapour fluctuations (q') and (f) net radiation (R_n), showing the occurrence of ramp patterns. This sample time series was collected on July 17, 2300 to 2315 hr (local time). For reference, we show a 1 m s^{-1} mean speed (dashed line).

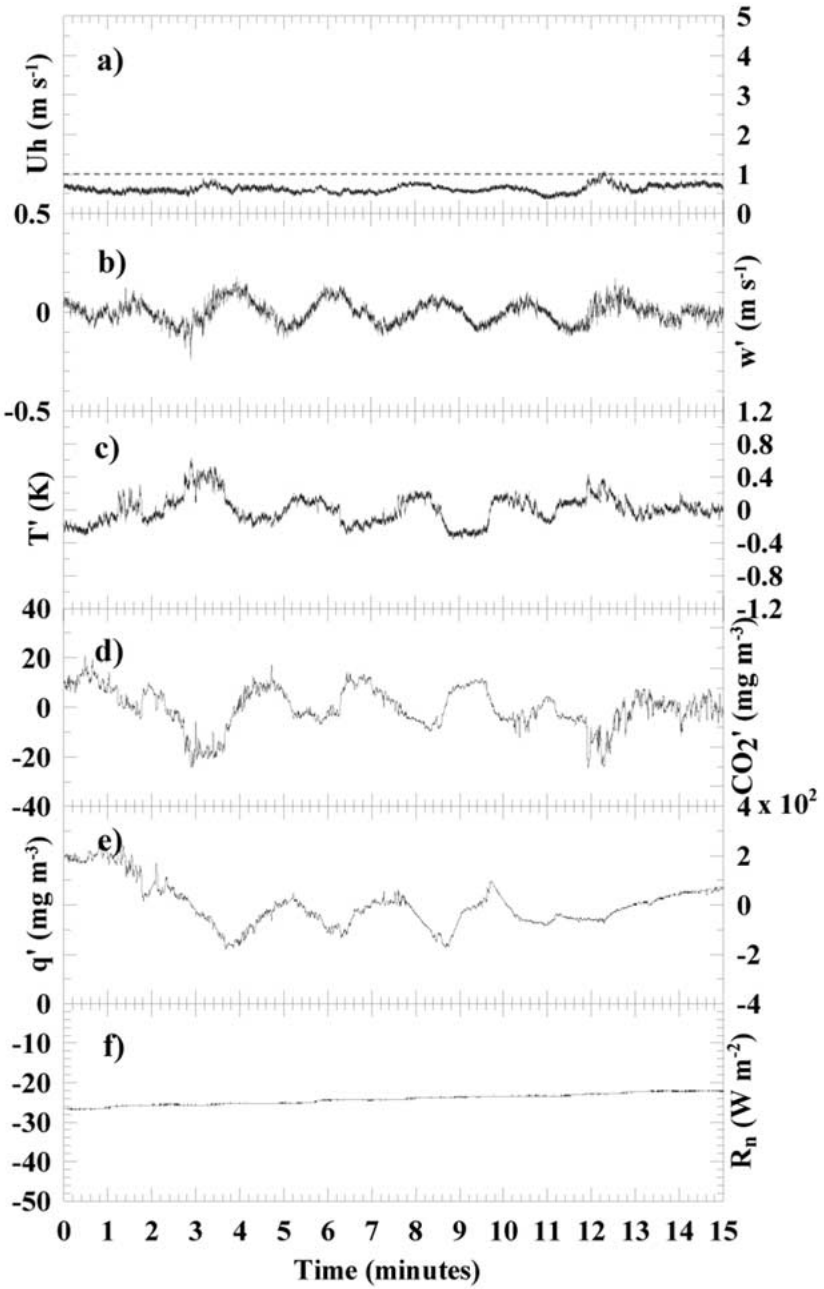

Figure 2. As in Figure 1, but showing the occurrence of canopy waves (class II). The time series was collected on July 7, 0300 to 0315 hr (local time). Note that the w' plot ranges between -0.5 and 0.5 m s^{-1}.

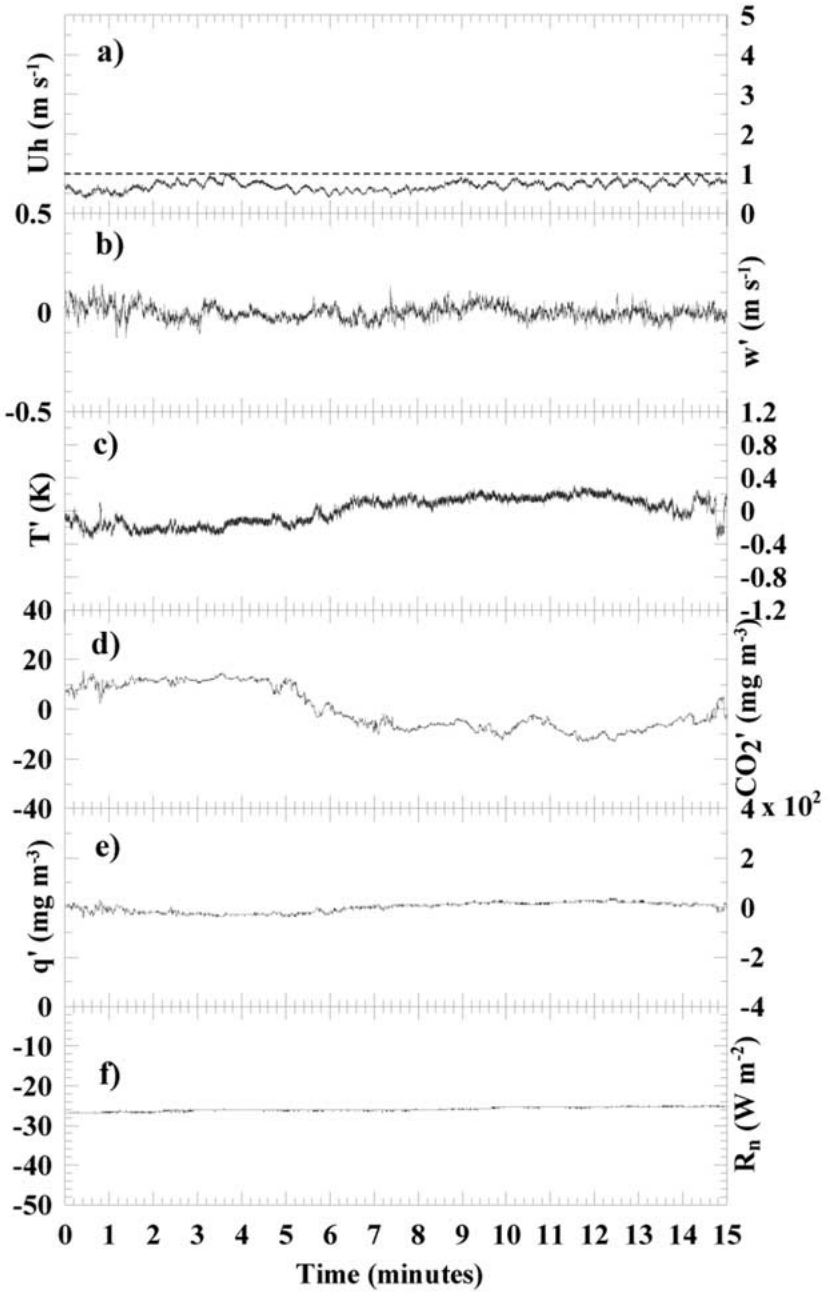

Figure 3. As in Figure 1, but showing a period where the flow lacked any organization and periodicity (fine-structure turbulence – class III). The time series was collected on July 13, 2315 to 2330 hr (local time). Note that the w' plot ranges between -0.5 and 0.5 m s^{-1}.

TABLE I

Summary of the percentage of occurrence during each analysed night for ramps (class I), canopy waves (class II), fine-structure turbulence (class III), period characterised by R_n variations exceeding 10 W m^{-2} and correlated with scalar pattern change (class IV), and periods characterised by an R_n variation greater than 10 W m^{-2} and not correlated with scalar pattern change (class V).

Night (Julian days)	% class I	% class II	% class III	% class IV	% class V
177–178	2.9	5.8	45.8	7.2	38.1
178–179	61.9	6.4	31.7	0	0
179–180	81.7	0	18.3	0	0
180–181	76.7	0	23.3	0	0
181–182	75.2	0	5.7	0	19.1
182–183	41.0	0	17.8	3.6	37.6
183–184	60.7	0	0	0	39.3
184–185	34.8	0	17.9	3.6	43.7
186–187	71.1	0	5.3	3.6	20.0
187–188	42.1	44.6	13.3	0	0
188–189	50.7	1.4	39.7	3.6	4.6
189–190	61.8	3.6	34.6	0	0
191–192	35.8	12.4	51.8	0	0
192–193	19.5	11.2	15.0	0	54.3
193–194	58.4	0	27.6	0	14.0
194–195	25.9	2.4	61.0	0	10.7
195–196	11.2	6.0	32.8	0	50.0
196–197	0.8	5.7	93.5	0	0
197–198	22.6	24.8	52.6	0	0
198–199	73.7	0	6.9	0	19.4
199–200	51.8	0	19.5	0	28.7
% mean	45.7	5.9	29.2	1.0	18.2

ation of organised structures resulted. Figure 4 shows the most representative of the six cases, where the abrupt change in all scalar patterns is clearly correlated to the increase in R_n (marked by the vertical dashed line). Note that the time constant of the net radiometer is much larger than that of the fast-response velocity and scalar sensors (i.e., 30 sec versus 0.1 sec). The strong variation in R_n (from -40 W m^{-2} to -6 W m^{-2}) produces periodic structures (very similar to ramps) characterised by a period of about 60–90 sec. The very low wind speed is an index of very weak mean shear at the canopy top. At such low wind speeds, Kelvin–Helmholtz instabilities cannot form, mechanical production of turbulent kinetic energy (TKE) is damped,

TABLE II

Parameters of interest relative to the six episodes belonging in class IV. The first column contains Julian day and time of each episode (the R_n variation occurs about in the centre of the period). In the other columns the undersigned b (or a) refers to statistics relative to the 15 min *before* (or *after*) the R_n variation; they contain the magnitude of the R_n variation (ΔR_n), the magnitudes of the ratio of momentum flux ($u'w'$), of sensible heat flux (Fs), of CO_2 flux (Fc) and of latent heat flux (Fl) before and after the R_n variation.

Julian day (time)	ΔR_n (W m^{-2}) (R_{nb}; R_{na}).	$(u'w')_a/(u'w')_b$	$(Fs)_a/(Fs)_b$	$(Fc)_a/(Fc)_b$	$(Fl)_a/(Fl)_b$
177	33.7	0.9	−2.6	8.1	19.5
(2030–2100)	(−39.4; −5.7)				
178	23.5	0.2	11.4	−31.3	6.5
(0020–0050)	(−27.6; −4.2)				
182	12.1	2.1	−0.5	0.9	0.5
(2145–2215)	(−30.3; −18.1)				
184	28.4	4.7	3.0	−15.5	3.8
(2155–2225)	(−30.6; −2.3)				
187	22.4	1.5	7.1	5.2	2.6
(0030–0100)	(−29.1; −6.8)				
189	14.0	1.7	1.8	2.9	2.4
(0030–0100)	(−45.8; −31.8)				

and hence radiative perturbations appear to be the dominant mode for production of TKE and scalar variances in the stable CSL. More important is that such radiative perturbations lead to high variability in scalar fluxes that appeared more pronounced than their momentum flux counterpart (see Table II). The strongest intensification of scalar fluxes occurs when $|\Delta R_n| > 20$ W m^{-2}. Another implication of the results in Figure 4 is that the passage of clouds introduces non-stationarity and care must be taken in linking measured fluxes to sources and sinks within the canopy volume.

Episodes belonging to class V are associated with a weakly stable atmosphere (usually $z/L < 1$) and occur usually with $|\Delta R_n| < 20$ W m^{-2}. Here, the mechanically produced turbulence is sufficiently large to sustain the ramp motion and radiative perturbations remain a second-order effect (at least when compared to ramps) as evidenced in Figures 4 and 5.

4.2. Spectral analysis

Figure 6 shows the mean spectra normalised by variances in wind velocity and scalars. The spectra are shown for periods dominated by ramps (class I), canopy waves (class II) and fine-structure turbulence (class III). The spectral peaks of

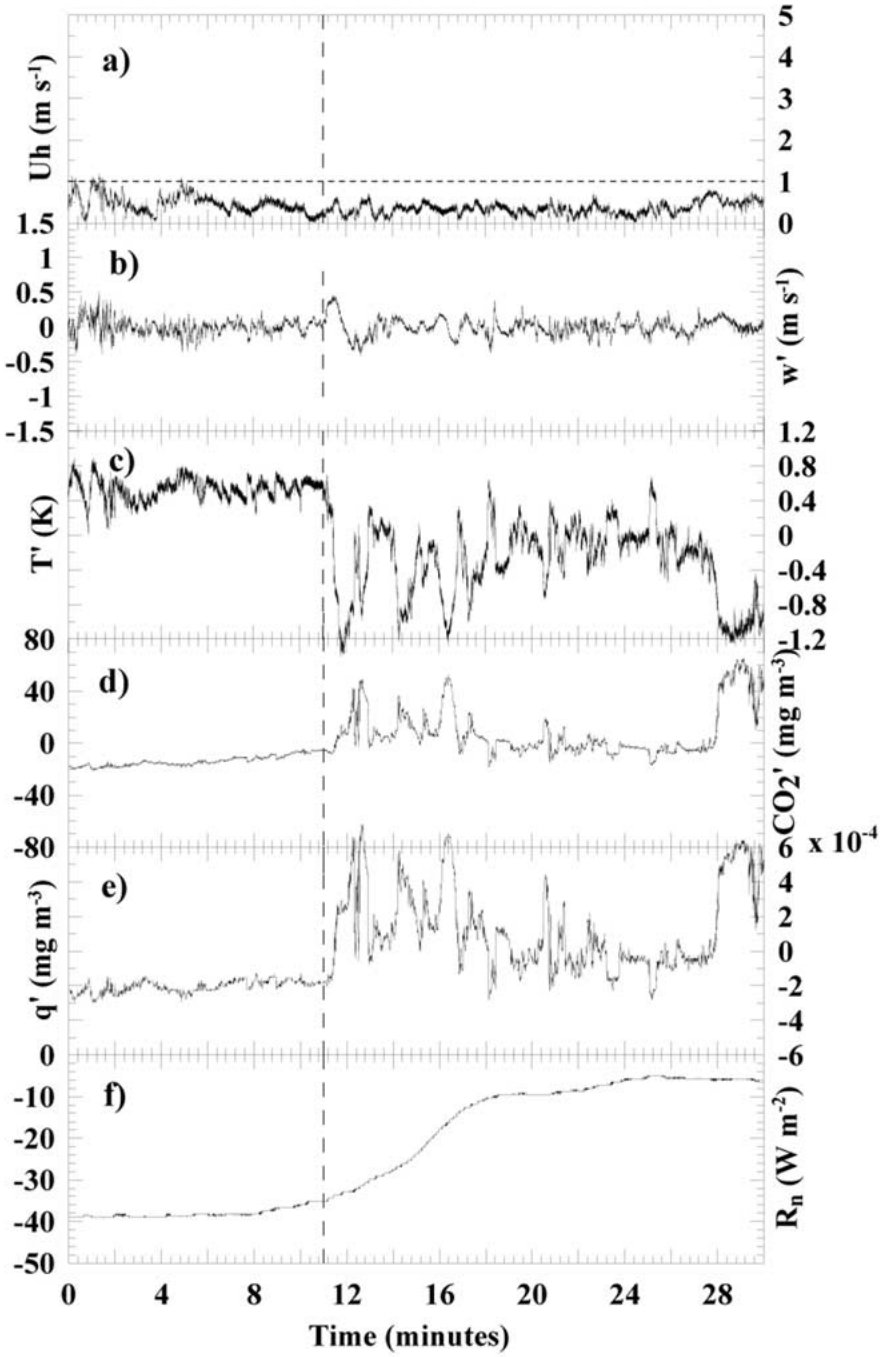

Figure 4. As in Figure 1, but showing the occurrence of an abrupt change in scalar patterns correlated with R_n variations (highlighted by the vertical dashed line) (class IV). The time series was collected on June 27, 2130 to 2200 hr (local time).

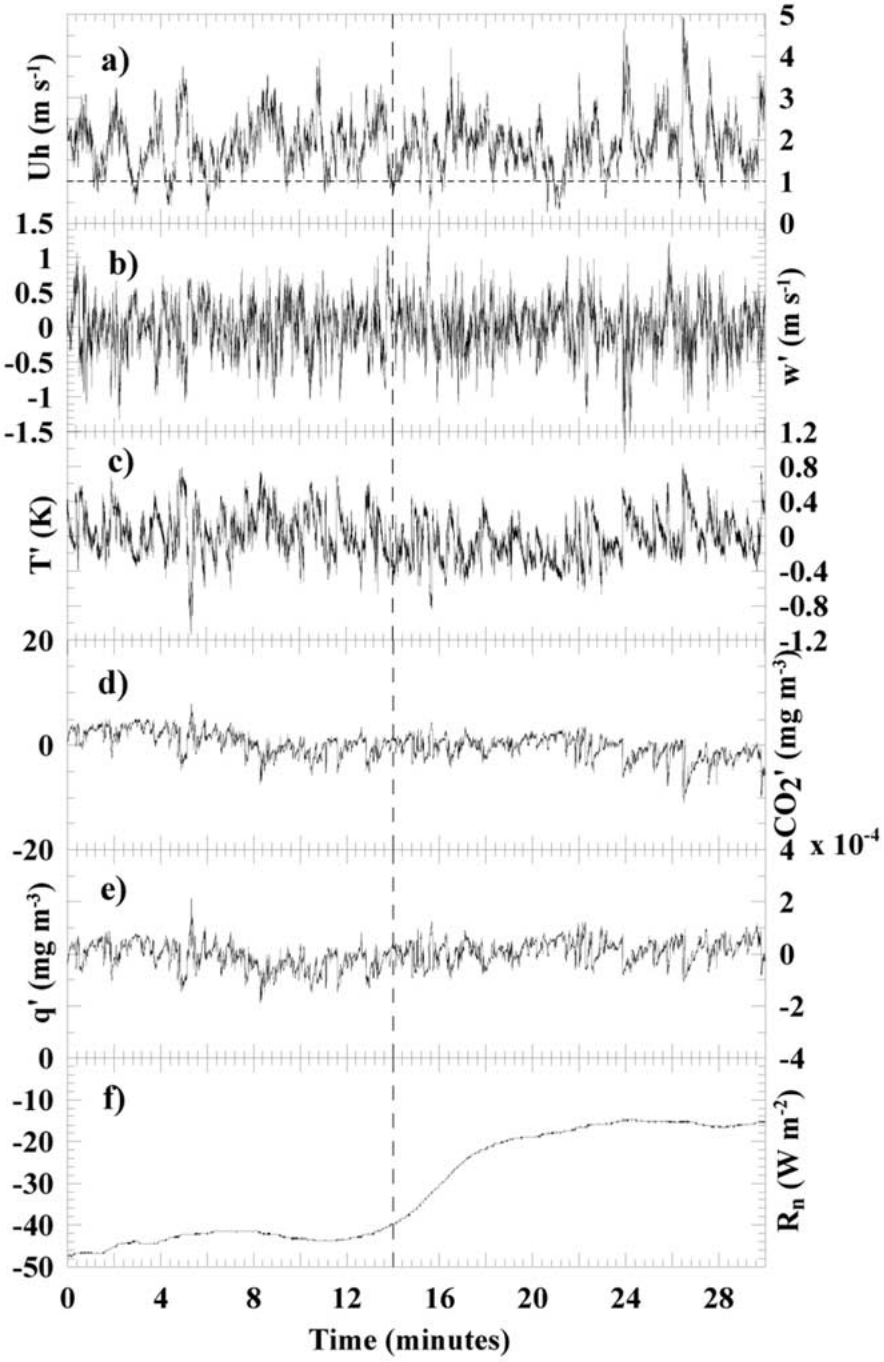

Figure 5. As in Figure 4, but showing the occurrence of an abrupt R_n variation (highlighted by the vertical dashed line) not correlated with any change in scalar patterns (class V). The time series was collected on July 12, 0200 to 0230 hr (local time).

ramps in u and scalars correspond to time scales of about 30–50 sec. The spectral maximum in the w component appears more shifted towards higher frequencies. In the inertial subrange, the roll-off of spectra of u and w is less steep than $f^{-2/3}$, whereas the roll-off rate of scalar spectra tends to be steeper.

The characteristic period of canopy waves deduced from spectral peaks is about 60–100 sec. Moreover spectra of velocity and scalars roll off as f^{-2} in the buoyancy subrange, and as $f^{-2/3}$ at frequencies higher than 0.1 Hz.

Cross-spectra of vertical velocity and scalars (Figures 7–9) confirm the different physical characteristics of ramp patterns and canopy waves and allow us to gain insight into the diffusive character of the different motions. Cross-spectra relative to class II (Figures 7b, 8b and 9b) reveal the typical characteristic of a pure linear wave field. In the region of the spectral peak (wave source region), the quad-spectrum exhibits a maximum, whereas the co-spectrum remains near zero; moreover, in the same region, the phase spectrum approaches $+90°$ for the $w-T$ cross-spectrum and $-90°$ for the $w-CO_2$ and w–q cross spectra. Finally the magnitude of the cospectral maximum highlights the different diffusive capability of ramps when compared to canopy waves and fine structure turbulence.

Episodes belonging in classes IV and V exhibit spectral characteristics (not shown) very similar to ramps (class I), but are noisier.

4.3. Autocorrelation function and integral time scales

Figures 10a and 10b show the mean autocorrelation function of w and T for each of the five classes of motions. Autocorrelation functions of CO_2 and q (not shown) exhibit behaviour similar to that of the T autocorrelation function.

Table III lists ensemble integral time scales for the five classes of motion. Note that they are in good agreement with the characteristic periods deduced by visual inspection of the time series and by spectral analysis. The w autocorrelation function for class II shows clear evidence of oscillation, indicating wave activity. Note the resemblance between the autocorrelation functions and integral time scales for classes V and I. This behaviour confirms that eddy motions belonging to class V are ramp patterns analogous to class I. Finally, the autocorrelation functions for classes II and IV tend to converge less rapidly, because they are often associated with non-stationary time series.

4.4. Statistical characterisation of detected events

Figure 11 shows the distribution of basic turbulent statistics for the five nocturnal CSL classes. We compare the first three classes to statistically characterise periods of near constant R_n. Not surprisingly, ramps appear to be associated with relatively strong winds, namely, periods dominated by mechanically produced turbulence and weak atmospheric stratification. About 60% of cases belonging in class I are characterised by $u > 1$ m s^{-1} and by $z/L < 1$. Canopy waves exist during periods of very stable atmospheric stability and low mean wind at the canopy-atmosphere

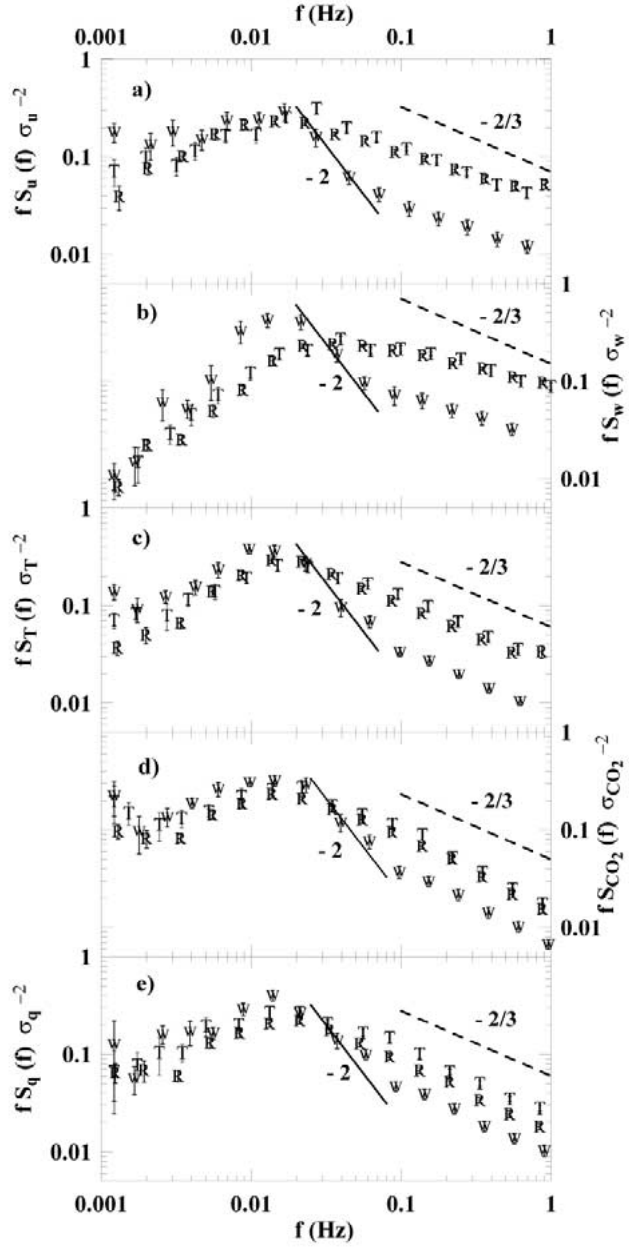

Figure 6. Mean spectra of (a) longitudinal velocity fluctuations (u'), (b) vertical velocity fluctuations (w'), (c) temperature fluctuations (T'), (d) CO_2 fluctuations and (e) water vapour fluctuations (q') for periods dominated by ramps (**R** $\rightarrow$ class I), canopy waves (**W** $\rightarrow$ class II) and fine-structure turbulence (**T** $\rightarrow$ class III). Dashed lines represent the $-2/3$ power law predicted from the Kolmogorov theory of the inertial subrange; continuous lines represent the -2 power law for the buoyancy subrange of gravity waves. Vertical bars represent the standard deviation around the mean (following ensemble averaging).

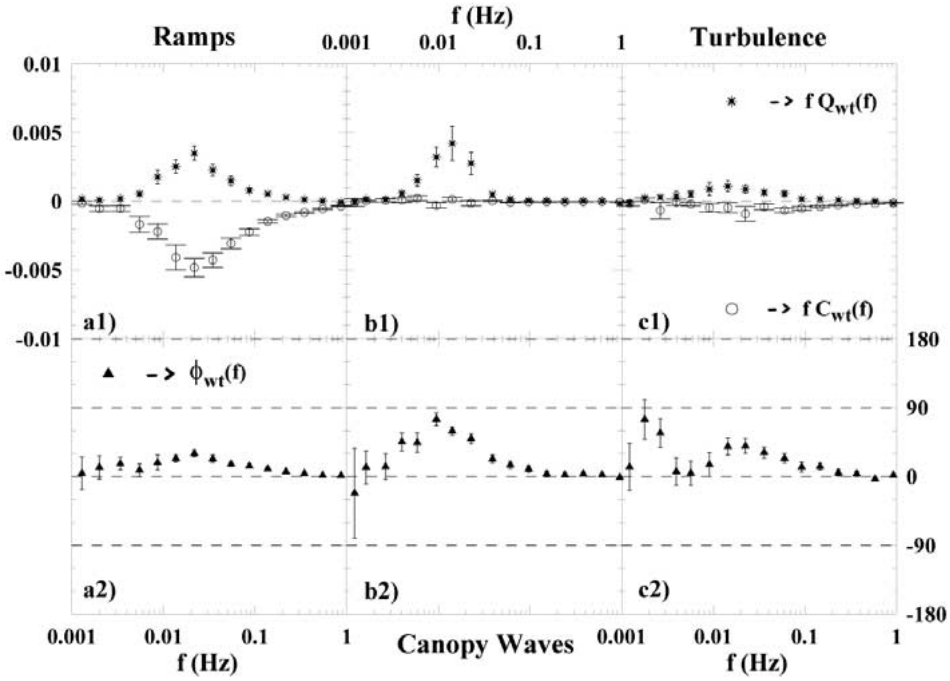

Figure 7. Mean cospectra (circles), mean quadrature spectra (stars) and mean phase spectra (triangles) of the vertical wind velocity fluctuations (w') and of the temperature fluctuations (T') for periods dominated by ramps (a1 and a2), canopy waves (b1 and b2), and fine-structure turbulence (c1 and c2). Vertical bars represent the standard deviation around the mean (following ensemble averaging).

TABLE III

Summary of the mean integral time scale (ITS) of the longitudinal velocity component (u), the vertical velocity component (w), the temperature (T), the CO_2, and the water vapour (q) relative to periods dominated by ramps (class I), canopy waves (class II), fine-structure turbulence (class III), period characterised by an R_n variation greater than 10 W m^{-2} and correlated with scalar pattern change (class IV), and period characterised by an R_n variation greater than 10 W m^{-2} and not correlated with scalar pattern change (class V). The uncertainty represents standard deviation around the mean.

Variable	Class I (sec)	Class II (sec)	Class III (sec)	Class IV (sec)	Class V (sec)
u	27 ± 2	100 ± 11	71 ± 4	53 ± 22	41 ± 4
w	10 ± 1	30 ± 2	17 ± 1	21 ± 7	13 ± 1
T	25 ± 1	61 ± 8	59 ± 3	48 ± 10	37 ± 3
CO_2	38 ± 2	67 ± 8	70 ± 4	64 ± 24	48 ± 3
q	44 ± 2	87 ± 10	82 ± 5	48 ± 7	51 ± 3

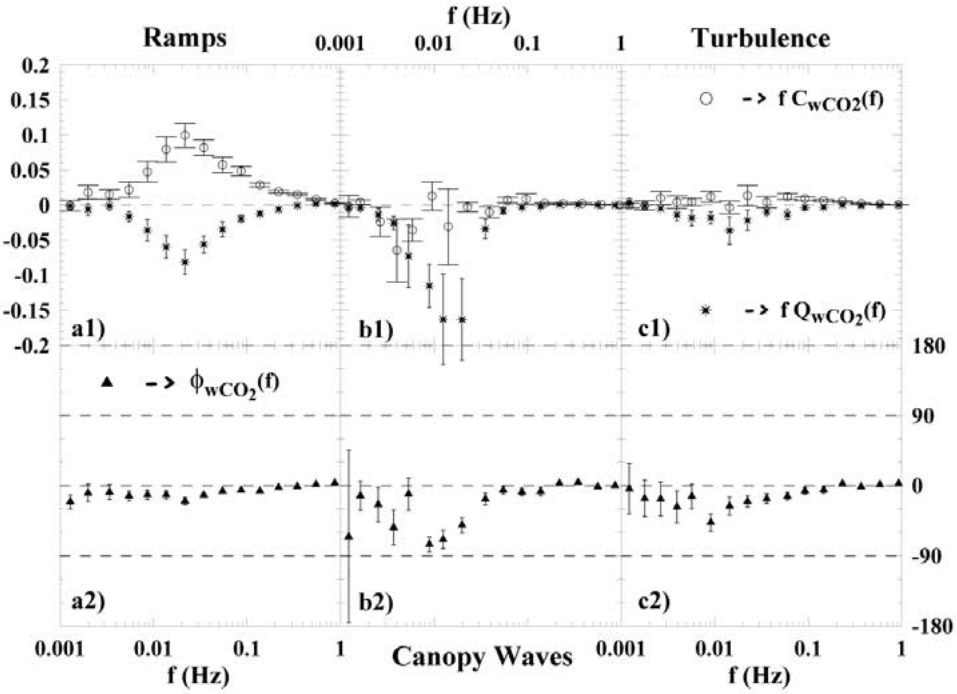

Figure 8. As in Figure 7, but for cross-spectra of the vertical velocity (w') and CO_2 fluctuations.

interface. For class II, the longitudinal wind speed never exceeds 1 m s^{-1}, and 65% of cases are characterised by $z/L > 1$. Analogous to ramps, canopy waves and turbulence are able to produce strong scalar fluctuations (cf. the distributions of scalar variances); nevertheless, they produce very low co-gradient (or sometimes counter-gradient) scalar fluxes. Counter-gradient fluxes and their linkage to canopy waves have been observed in a previous experimental study (cf. Lee et al., 1996).

Organised structures induced or 're-vitalised' by radiative instability such as the passage of clouds (class IV) tend to reduce atmospheric stability and greatly enhance scalar fluxes. For class IV, the variance and flux values often are at the tail of ramp distributions. In some cases, counter-gradient fluxes have been observed. The similarity of distributions in classes V and I also confirms that cloud cover variations do not perturb the structure of the nocturnal CSL in the presence of well-developed ramp patterns.

Finally, Figure 12 summarises the transport efficiency of the five selected classes of motions. It is evident that CO_2 and other passive scalars are mainly transported by ramps (classes V and I). Even if linear canopy waves remain active for 50% of the night, they are unable to contribute to the net transport of scalars.

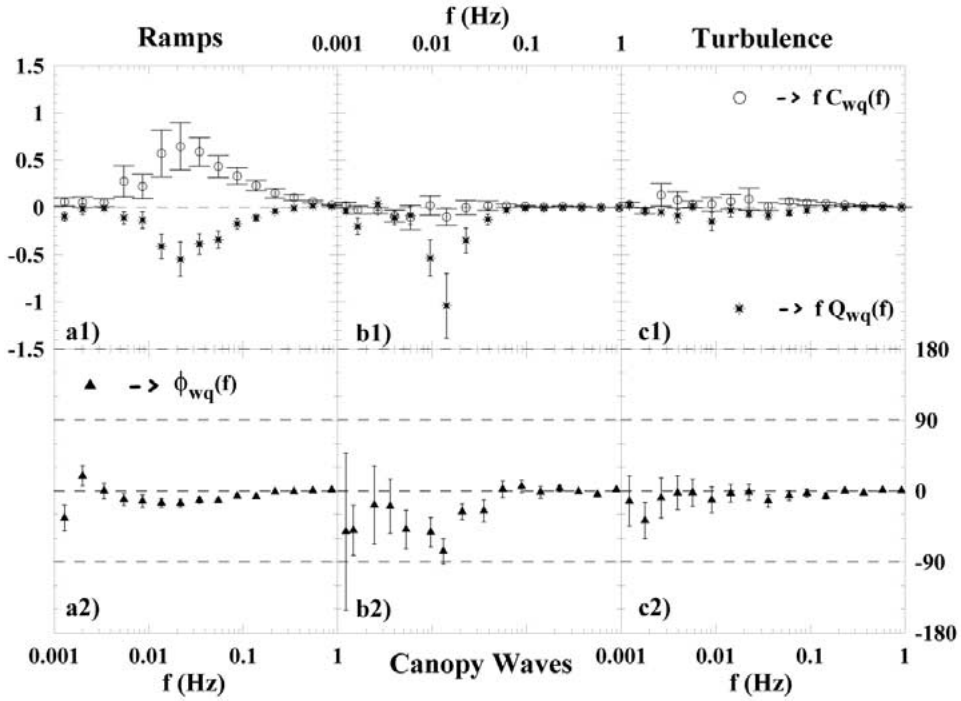

Figure 9. As in Figure 7, but for cross-spectra of the vertical velocity (w') and water vapour (q') fluctuations.

5. Conclusions

The structure of the nocturnal CSL close to the canopy-atmosphere interface of an even-aged pine forest was investigated using time series measurements of velocity and scalars with varying sources and sinks within the canopy volume. Primarily, we focused on identifying different classes of organised motion and their role in scalar transport. Our analysis demonstrated the following:

(1) During clear sky nights both ramp patterns and linear canopy waves have been observed. Ramps occur most frequently during the night; their characteristic period is about 30–60 sec; moreover they are associated with a relatively high mean wind speed ($u > 1$ m s^{-1}) and weak thermal stratification ($z/L < 1$).

(2) Observed canopy waves appear during periods of very stable atmospheric stability (usually $z/L \gg 1$) and possess a dominant period of 60–120 sec similar to that observed in other experimental studies.

(3) Although ramps and canopy waves possess different periods, they appear to be characterised by roughly the same spatial scale (30–60 m) consistent with the study of Brunet and Irvine (2000).

(4) Canopy waves occasionally populate 50% of the night; however, cross-spectral analysis demonstrated that their net mass exchange of scalars is nearly zero.

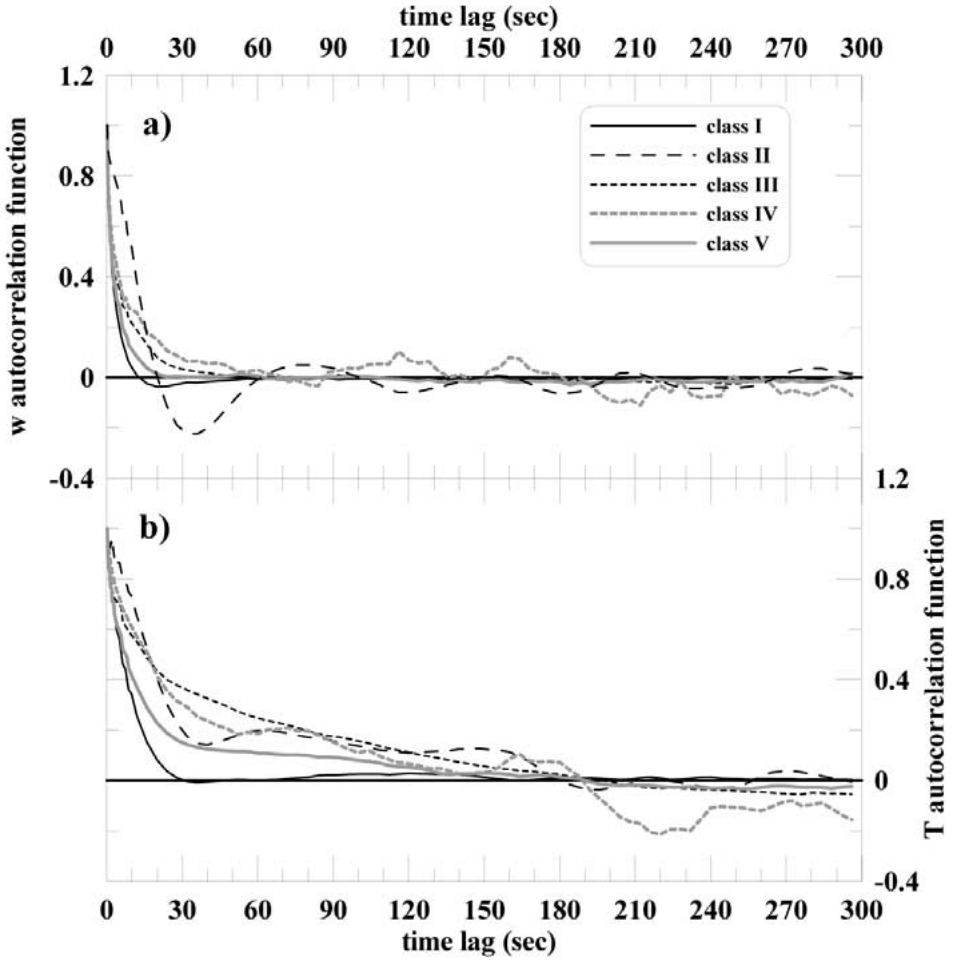

Figure 10. Mean autocorrelation function of the vertical velocity component (a) and of temperature (b), for periods dominated by ramps (class I), canopy waves (class II), fine-structure turbulence (class III), period characterised by R_n variation exceeding 10 W m^{-2} and correlated with scalars (class IV), and period characterised by an R_n variation greater than 10 W m^{-2} and not correlated with scalar time series (class V).

Small counter-gradient fluxes produced by canopy waves depend on small deviations from $\pm 90^{\circ}$ of the phase angle between vertical velocity and scalar (Lee et al., 1996) also observed here.

(5) During cloudy nights, radiative effects can significantly perturb the nocturnal CSL above the forest. The passage of clouds increases net radiation (i.e., making it less negative) thereby producing (or intensifying) organised structures. These structures possess time scales and structural features similar to the ramp-like motions. We clearly observed abrupt changes in scalar flux patterns and a strong intensification of scalar fluxes when $|\Delta R_n| > 20$ W m^{-2} and

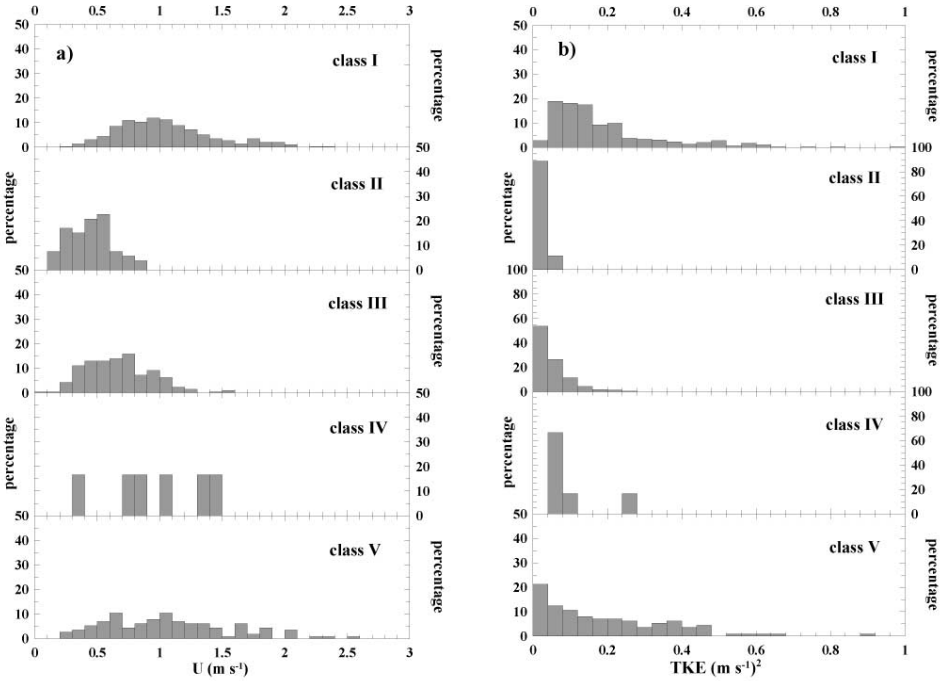

Figure 11a,b. Distribution of the mean wind (a) and turbulent kinetic energy ($= \frac{1}{2}\overline{u_i' u_i'}$) (b) for periods characterized by ramps (class I), canopy waves (class II), fine-structure turbulence (class III), period characterised by an R_n variation greater than 10 W m^{-2} and correlated with scalar pattern change (class IV), and period characterised by an R_n variation greater than 10 W m^{-2} and not correlated with scalar pattern change (class V).

when pre-existing strong stable stratification dominated such periods. In near-neutral to slightly stable atmospheric conditions that are dominated by intense shear stress levels, radiative perturbations do not profoundly perturb the ramp patterns.

In short, the emerging picture from our analysis is that the nocturnal CSL has two end-members, both dominated by organised motions (Figure 13). These end-members represent fully developed turbulence for near-neutral and slightly stable flows, to zero turbulence in very stable conditions ($z/L \gg 1$). Ramps dominate scalar transport for near-neutral and slightly stable conditions and canopy waves dominate the flow dynamics for very stable conditions. Cospectral analysis suggest that ramps are the most efficient net mass transporting agent while canopy waves contribute little to net scalar transport between the canopy and atmosphere. Numerous night-time runs reside between these two end-members and are characterized by fine-scale and damped turbulence. If radiative perturbations are sufficiently large (>20 W m^{-2} in net radiation), the flow can switch from being damped and

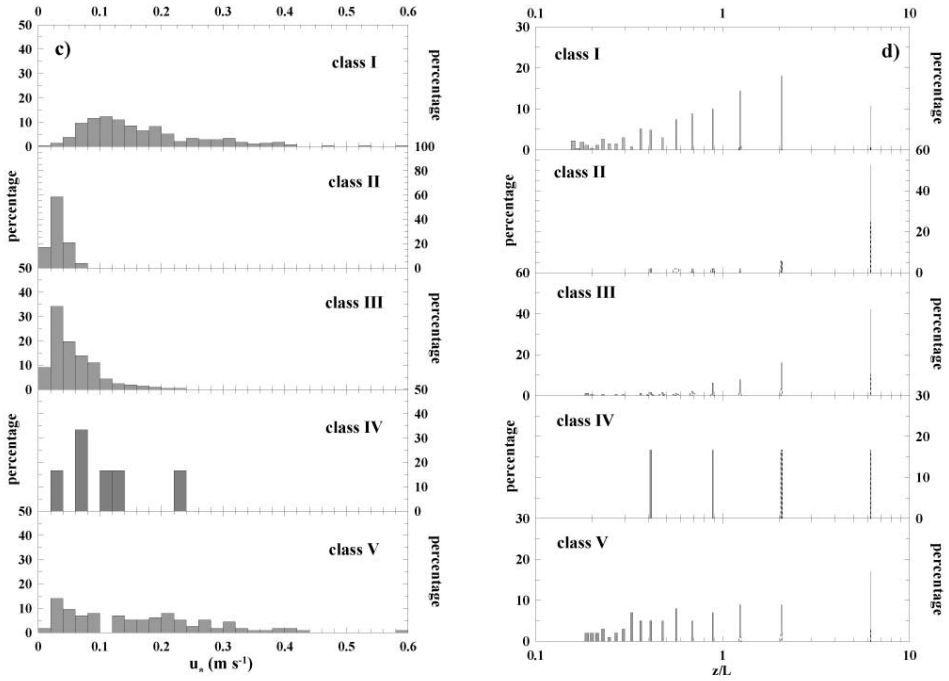

Figure 11c,d. As Figure 11a,b, but for friction velocity (c) and z/L (d). In Figure 11d the dotted bars refer to negative value of z/L.

governed by random fine-scale turbulence to organised turbulence with ramp-like features.

The broader implication is that night-time CO_2 flux corrections, now routinely used across all FluxNet sites (e.g., Falge et al., 2002; Barford et al., 2001), can take better advantage of such classifications. Large friction velocity (u_*) thresholds usually filter runs associated with canopy waves or other non-stationary intermediate states between the two members proposed here. It is clear that when canopy waves dominate night-time runs, the local CO_2 production from ecosystem respiration and observed mean fluxes above the canopy are, to a first order, de-coupled presumably through a large storage term. What is important here is that when canopy waves dominate, there is 'gross' mass and heat exchange between the canopy and the atmosphere; however, the net exchange over the life cycle of the wave is negligible. Occasionally, these waves are under-sampled because of a short flux-averaging period leading to an apparent and spurious 'photosynthesis' (or canopy C uptake) values at night in the case of CO_2. Correcting night-time fluxes with runs collected under high u_* (or more precisely for near-neutral to slightly stable conditions) ensures that the turbulent regime is fully-developed and ramps are likely to dominate the scalar exchange process. For such conditions, it is clear that the TKE and the coupling between sources and fluxes are large. Another reason why runs with high

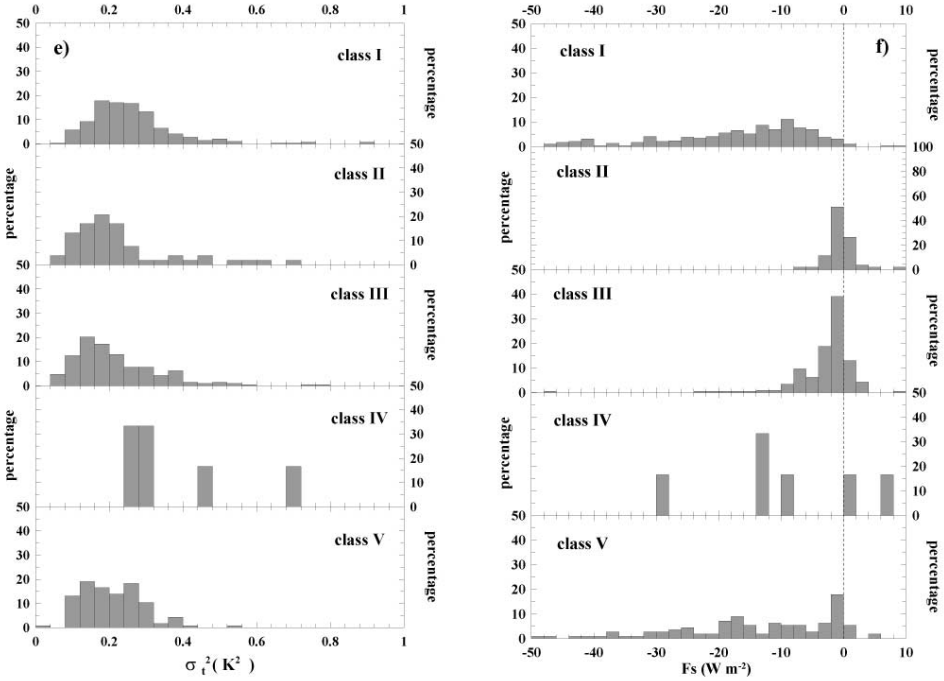

Figure 11e,f. As Figure 11a,b, but for temperature variance (e) and sensible heat flux (f).

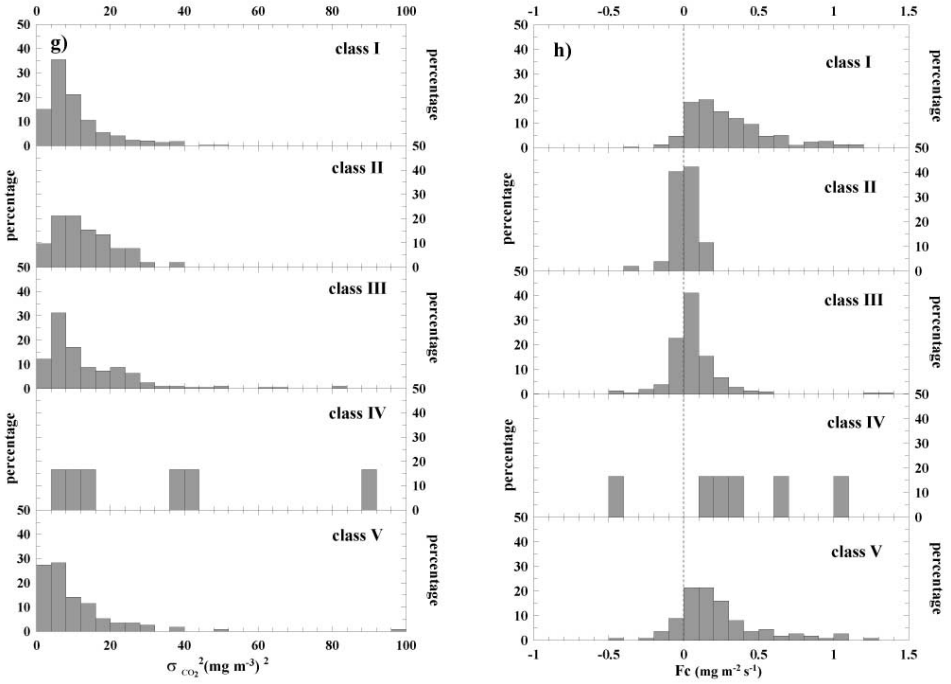

Figure 11g,h. As Figure 11a,b, but for CO_2 variance (g) and CO_2 flux (h).

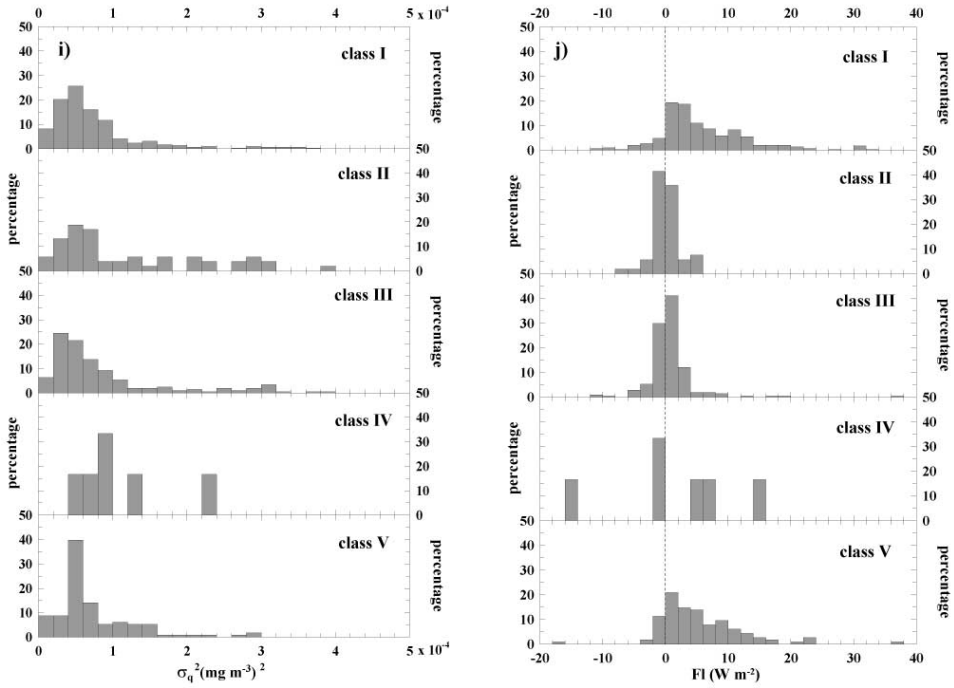

Figure 11i,j. As Figure 11a,b, but for water vapour variance (i) and latent heat flux (j).

u_* (or near-neutral conditions) are preferred for night-time flux corrections is that such runs have a much smaller (and perhaps the more realistic) footprint.

Acknowledgements

The authors would like to thank John Albertson and Michael Raupach for their helpful comments and discussions. The first two authors acknowledge the Italian MURST Project 'Sviluppo di tecnologie innovative e di processi biotecnologici in condizioni controllate nel settore delle colture vegetali: Diagnosi e Prognosi di situazioni di stress idrico per la vegetazione'. The third author acknowledges the support by 'Conselho Nacional de Desenvolvimento Científico e Tecnológico' (CNPq) of Brazil. The last author acknowledges support from the Center on Global Change (Duke University) during his leave in the autumn of 2002. Additional support was provided by the National Science Foundation (NSF-EAR-99-03471 and -DMS-00-72585), the Biological and Environmental Research (BER) Program, U.S. Department of Energy, through the south-east Regional Center (SERC) of the National Institute for Global Environmental Change (NIGEC), and through the Terrestrial Carbon Processes Program (TCP) and the FACE project.

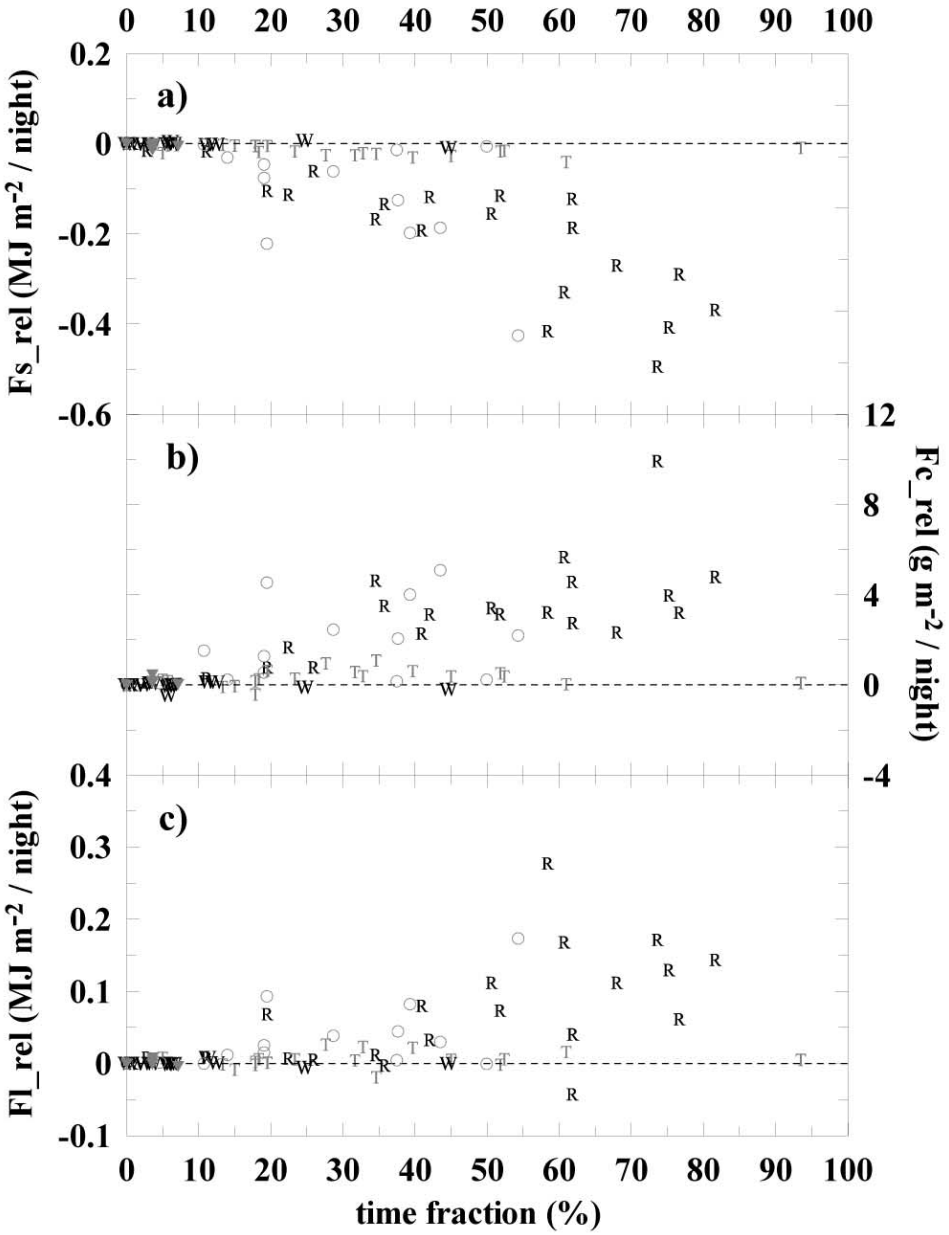

Figure 12. Integral nocturnal contribution to the sensible heat flux (a), to the latent heat flux (b) and to the CO_2 flux by ramps (**R** → class I), canopy waves (**W** → class II), fine-structure turbulence (**T** → class III), period characterised by an R_n variation greater than 10 W m^{-2} and correlated with scalar pattern change (triangles → class IV), and period characterised by an R_n variation greater than 10 W m^{-2} and not correlated with scalar pattern change (circles → class V).

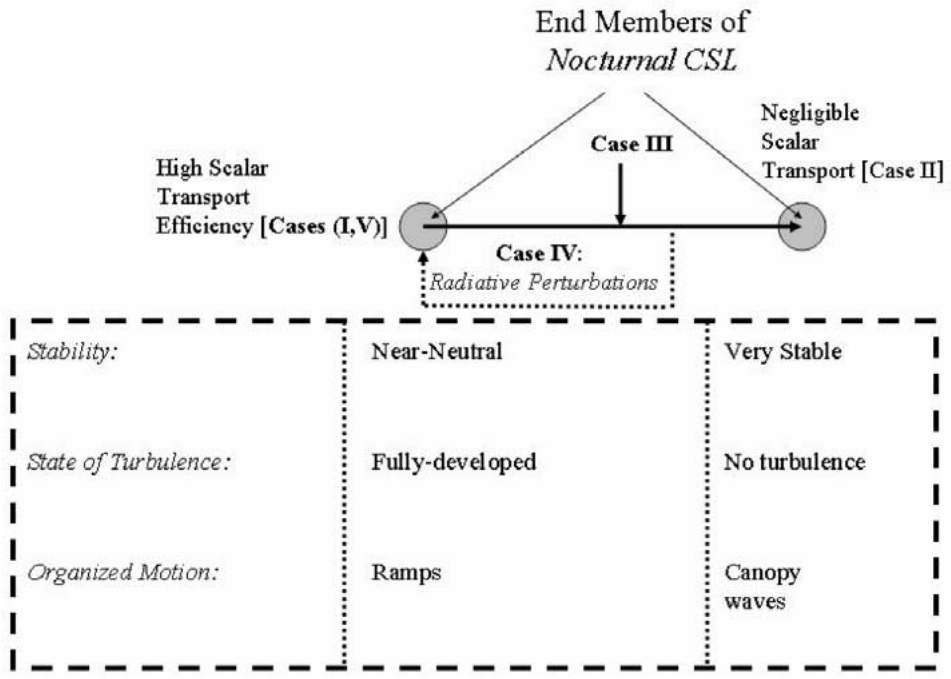

Figure 13. End-members of organized motion in the nocturnal CSL. One end-member is dominated by ramps, fully developed turbulence, efficient scalar net exchange between the canopy and the atmosphere, and near-neutral to slightly stable stability conditions. The other end-member is dominated by linear canopy waves, no turbulence, negligible net scalar exchange, and very stable conditions. All other cases are between these two end-members. Intermediate cases are dominated by fine-scale and damped turbulence. Radiative perturbations (e.g., Case IV) can shift these intermediate cases to ramp-like motion. Any complete theory for the nocturnal CSL must recover these two end-members and transitions between them for different stability classes and radiative perturbations.

References

Baldocchi, D. D., Falge, E., Gu, L., Olson, R., Hollinger, D., Running, S., Anthoni, P., Bernhofer, Ch., Davis, K., Fuentes, J., Goldstein, A., Katul, G., Law, B., Lee, X., Malhi, Y., Meyers, T., Munger, J. W., Oechel, W., Pilegaard, K., Schmid, H. P., Valentini, R., Verma, S., Vesala, T., Wilson K., and Wofsy, S.: 2001, 'FLUXNET: A New Tool to Study the Temporal and Spatial Variability of Ecosystem-Scale Carbon Dioxide, Water Vapour and Energy Flux Densities', *Bull. Amer. Meteorol. Soc.* **82**, 2415–2435.

Barford, C.C., Wofsy, S.C., Goulden, M. L., Munger, J. W., Pyle, E. H., Urbanski, S. P., Hutyra, L., Saleska, S. R., Fitzjarrald, D., and Moore, K.: 2001, 'Factors Controlling Long- and Short-Term Sequestration of Atmospheric CO_2 in a Mid-Latitude Forest', *Science* **294**, 1688–1691.

Bergström, H. and Högstrom, U.: 1989, 'Turbulent Exchange above a Pine Forest. II Organised Structures', *Boundary-Layer Meteorol.* **49**, 231–263.

Bergström, H. and Smedman, A. S.: 1994, 'Stably Stratified Flow in a Marine Atmospheric Surface Layer', *Boundary-Layer Meteorol.* **72**, 239–265.

Brunet, Y. and Irvine, M. R.: 2000, 'The Control of Coherent Eddies in Vegetation Canopies: Streamwise Structure Spacing, Canopy Shear Scale and Atmospheric Stability', *Boundary-Layer Meteorol.* **94**, 139–163.

Brunet, Y. and Collineau, S.: 1994, 'Wavelet Analysis of Diurnal and Nocturnal Turbulence above a Maize Crops', in Efi Foufoula-Georgiou and Praveen Kumar (eds.), *Wavelet in Geophysics*, Academic Press, Inc., pp. 129–150.

Bush, N. E.: 1969, 'Waves and Turbulence', *Radio Sci.* **4**, 1377–1379.

Caughey, S. J.: 1977, 'Boundary-Layer Turbulence Spectra in Stable Conditions', *Boundary-Layer Meteorol.* **11**, 3–14.

Caughey, S. J. and Readings, C. J.: 1975, 'An Observation of Waves and Turbulence in the Earth's Boundary Layer', *Boundary-Layer Meteorol.* **9**, 279–296.

Collineau, S. and Brunet, Y.: 1993, 'Detection of Turbulent Coherent Motions in a Forest Canopy, Part II: Timescales and Conditional Averages', *Boundary-Layer Meteorol.* **66**, 49–73.

de Baas, A. F. and Driedonks, G. M.: 1985: 'Internal Gravity Waves in a Stably Stratified Boundary Layer', *Boundary-Layer Meteorol.* **31**, 303–323.

Falge, E., Baldocchi, D., Tenhunen, J., Aubinet, M., Bakwin, P., Berbigier, P., Bernhofer, C., Burba, G., Clement, R., Davis, K. J., Elbers, J. A., Goldstein, A. H., Grelle, A., Granier, A., Guomundsson, J., Hollinger, D., Kowalski, A. S., Katul, G., Law, B. E., Malhi, Y., Meyers, T., Monson, R. K., Munger, J. W., Oechel, W., Paw, K. T., Pilegaard, K., Rannik, U., Rebmann, C., Suyker, A., Valentini, R., Wilson, K., and Wofsy, S.: 2002, 'Seasonality of Ecosystem Respiration and Gross Primary Production as Derived from FLUXNET Measurements', *Agric. For. Meteorol.* **113**, 53–74.

Finnigan, J. J.: 2000, 'Turbulence in Plant Canopies', *Annu. Rev. Fluid Mech.* **32**, 519–571.

Fitzjarrald, D. R. and Moore, K. E.: 1990, 'Mechanisms of Nocturnal Exchange between the Rain Forest and the Atmosphere', *J. Geophys. Res.* **95D**, 16839–16850.

Gao, W., Shaw, R. H., and Paw U, K. T.: 1989, 'Observation of Organised Structures in Turbulent Flow within and above a Forest Canopy', *Boundary-Layer Meteorol.* **47**, 349–377.

Garratt, J. R.: 1992, *The Atmospheric Boundary Layer*, Cambridge University Press, Cambridge, U.K., 316 pp.

Hu, X., Lee, X., Stevens, D. E., and Smith, R. B.: 2002, 'A Numerical Study of Nocturnal Wavelike Motion in Forests', *Boundary-Layer Meteorol.* **102**, 199–223.

Hunt, J. C. R., Kaimal, J. C., and Gaynor, J. E.: 1985, 'Some Observations of Turbulence Structure in a Stable Layer', *Quart. J. Roy. Meteorol. Soc.* **111**, 793–815.

Jenkins, G. M. and Watts, D. G.: 1968, in *Spectral Analysis and its Applications*, Holden-Day, Oackland, pp. 344–348.

Katul, G. and Vidakovic, B.: 1998, 'Identification of Low-Dimensional Energy Containing/Flux Transporting Eddy Motion in the Atmospheric Surface Layer Using Wavelet Thresholding Methods', *J. Atmos. Sci.* **55**, 377–389.

Katul, G. G., Geron, C. D. Hsieh, C. I. Vidakovic, B., and Guenther, A. B.: 1998, 'Active Turbulence and Scalar Transport near the Land-Atmosphere Interface', *J. Appl. Meteorol.* **37**, 1533–1546.

Katul, G. G., Hsieh, C. I. Kuhn, G., Ellsworth, D., and Nie, D.: 1997, 'The Turbulent Eddy Motion at the Forest-Atmosphere Interface', *J. Geophys. Res.* **102**, 13409–13421.

Kolmogorov, A. N.: 1941, 'The Local Structure of Turbulence in Incompressible Viscous Fluid for Very Large Reynolds Number', *Dokl. Akad. Nauk. SSSR* **30**, 9–13.

Lai, C. T., Katul, G. G., Butnor, J., Siqueira, M., Ellsworth, D., Maier, C., Johnsen, K., McKeand, S., and Oren, R.: 2002, 'Modeling the Limits on the Response of Net Carbon Exchange to Fertilization in a Southeastern Pine Forest', *Plant Cell Environ.* **25**, 1095–1119.

Lee, X.: 1997, 'Gravity Waves in a Forest: A Linear Analysis', *J. Atmos. Sci.* **54**, 2574–2585.

Lee, X. and Barr, A. G.: 1998, 'Climatology of Gravity Waves in a Forest', *Quart. J. Roy. Meteorol. Soc.* **124**, 1403–1419.

Lee, X., Black, T. A., den Hartog, G., Neumann, H. H., Nesic, Z., and Olejnik, J.: 1996, 'Carbon Dioxide Exchange and Nocturnal Processes over a Mixed Deciduous Forest', *Agric. For. Meteorol.* **81**, 13–29.

Lee, X., Neumann, H. H., den Hartog, G., Fuentes, J. D., Black, T. A., Mickle, R. E., Yang, P. C., and Blanken, P. D.: 1997, 'Observation of Gravity Waves in a Boreal Forest', *Boundary-Layer Meteorol.* **84**, 383–398.

Mahrt, L.: 1999, 'Stratified Atmospheric Boundary Layers', *Boundary-Layer Meteorol.* **90**, 375–396.

McMillen, R. T.: 1988, 'An Eddy Correlation Technique with Extended Applicability to Non-Simple Terrain', *Boundary-Layer Meteorol.* **43**, 231–245.

Nai-Ping, L., Neff, W. D., and Kaimal, J. C.: 1983, 'Waves and Turbulence Structure in a Disturbed Nocturnal Inversion', *Boundary-Layer Meteorol.* **26**, 141–155.

Nappo, C. J.: 1991: 'Sporadic Breakdowns of Stability in the PBL over Simple and Complex Terrain', *Boundary-Layer Meteorol.* **54**, 69–87.

Paw U, K. T., Brunet, Y., Collineau, S., Shaw, R. H., Maitani, T., Qiu, J., and Hipps, L.: 1992, 'On Coherent Structures in Turbulence above and within Agricultural Plant Canopies', *Agric. For. Meteorol.* **61**, 55–68.

Press, W. H., Vetterling, W., Teukolsky, S., and Flannery, B.: 1992, *Numerical Recipes in Fortran*, Cambridge University Press, 962 pp.

Raupach, M. R. and Thom, A. S.: 1981, 'Turbulence in and above Plant Canopies', *Annu. Rev. Fluid Mech.* **13**, 97–129.

Raupach, M. R., Finnigan, J. J., and Brunet, Y.: 1996, 'Coherent Eddies and Turbulence in Vegetal Canopies: The Mixing Layer Analogy', *Boundary-Layer Meteorol.* **78**, 351–382.

Shaw, R. H., Paw U, K. T., and Gao, W.: 1989, 'Detection of Temperature Ramps and Flow Structures at a Deciduous Forest Site', *Agric. For. Meteorol.* **47**, 123–138.

Siqueira, M. B., Katul, G. G., and Lai, C. T.: 2002, 'Quantifying Net Ecosystem Exchange by Multilevel Ecophysiological and Turbulent Transport Models', *Adv. Water Resour.* **25**, 1357–1366.

Smedman, A. S.: 1988, 'Observation of a Multi-Level Turbulence Structure in a Very Stable Atmospheric Boundary Layer', *Boundary-Layer Meteorol.* **44**, 231–253.

Stewart, R. W.: 1969, 'Turbulence and Waves in a Stratified Atmosphere', *Radio Sci.* **4**, 1269–1278.

Stull, R.: 1988, *An Introduction to Boundary Layer Meteorology*, Kluwer Academic Publishers, Dordrecht, 666 pp.

Valentini, R., Matteucci, G., Dolman, A. J., Schulze, E. D., Rebmann, C., Moors, E. J., Granier, A., Gross, P., Jensen, N. O., Pilegaard, K., Lindroth, A., Grelle, A., Bernhofer, C., Grunwald, T., Aubinet, M., Ceulemans, R., Kowalski, A. S., Vesala, T., Rannik, U., Berbigier, P., Loustau, D., Guomundsson, J., Thorgeirsson, H., Ibrom, A., Morgenstern, K., Clement, R., Moncrieff, J., Montagnani, L., Minerbi, S., and Jarvis, P. G.: 2000, Respiration as the Main Determinant of Carbon Balance in European Forests', *Nature* **404**, 861–865.